Electrified cloud areas observed in the SHV and LDR radar modes

Valery Melnikov*+ and Dusan Zrnic+
*-CIMMS, the University of Oklahoma, +- NOAA/OAR National Severe Storms Laboratory

Dual polarization radars are capable of observing areas of canted ice crystals aligned by strong in-cloud electric fields. Such areas have been observed using radars with circular (McCormic and Hendry 1976, Hendry and Antar 1982, Furuta et al. 1985, Krehbiel et al. 1991, 1992, 1996; Metcalf 1995), alternate (Caylor and Chandrasekar 1996, Caylor et al. 1993), simultaneous (Ryzhkov and Zrnic 2007, Melnikov et al. 2009, Hubbert et al. 2014, Biggerstaff et al.2017, Weber et al. 2017) polarizations as well as in measurements of linear depolarization ratio, LDR mode (Melnikov et al., 2009). Canted ice crystals strongly depolarize return radar signals and therefore one can expect to observe the depolarization effects more clearly with radars operating in the LDR or circular polarizations modes. The most popular polarization mode nowadays is one with Simultaneous transmission and reception of Horizontally and Vertically polarized waves (SHV mode). To compare the capabilities of the SHV and LDR modes in detecting areas of aligned crystals, we have ran these modes sequentially on the research-and-development WSR-88D KOUN located at Norman, OK.

In 2006-2008, KOUN had a capability of switching between the SHV and LDR modes and collecting data separated by about 3-4 min. In the SHV mode, the radar variables were reflectivity (Z), Doppler velocity (V), spectrum with (W), differential reflectivity (Z_{DR}), differential phase (Φ_{DP}), and copolar correlation coefficient (ρ_{hv}). In the LDR mode, Z, V, W, linear depolarization ratio (L_{DR}), differential phase (Φ_{XP}), and cross-polar correlation coefficient (ρ_{xh}) were measured. In the LDR mode, transmitted polarization was horizontal. To compare the fields of radar variables, vertical cross sections (RHI) through cores of thunderstorms were made in the sequence SHV-LDR-SHV. Data from the first and last SHV modes were used to assure that a thunderstorm did not change its structure significantly. Then the radar fields from the SHV and LDR modes were compared.

An example is shown in Fig. 1, where Z field is the same for both modes and polarization variables are show in two rows: the first is from the SHV mode and the lower is from the LDR mode. The differential phases are presented in degrees. In LDR mode, Φ_{XP} fluctuates widely for primarily horizontally oriented scatterers. The fuzzy yellow-red-black areas in the Φ_{XP} field in Fig. 1 contain primarily horizontally oriented scatterers. Areas with canted particles exhibit much uniform values of the phase (see the green areas in the Φ_{XP} panel). The Φ_{XP} values depend on many particles' properties as well as on the radar viewing angle. Therefore, to select zones with canted particles, we should just look for areas of uniform Φ_{XP} values. Comparing Z_{DR} and L_{DR} fields we note the presence of negative Z_{DR} and enhanced L_{DR} values at the top of thunderstorm, which both point to the presence of canted particles. This conclusion is supported by negative Φ_{DP} in the area. We also see that area of uniform Φ_{XP} is much larger than that of Φ_{DP}. Also note a greenish area at distances from 30 to 60 km and at heights higher than 10 km in the trailing MCS system. We can suppose that there also are electric fields capable of canting the particles. The ρ_{hv} field has no features in the areas of interest whereas ρ_{xh} field shows a large area of high values, which also points to the presence of canted particles.

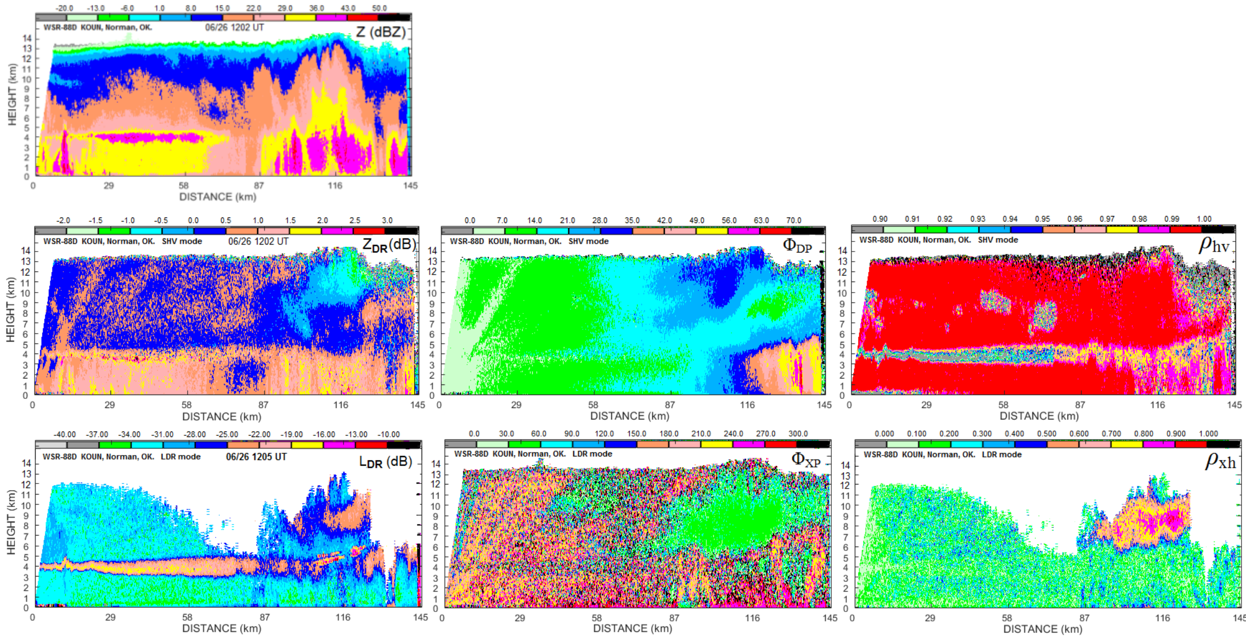

Fig. 1. RHIs collected on 26 June 2007 at 1202 UTC at an azimuth of 209^{o}.

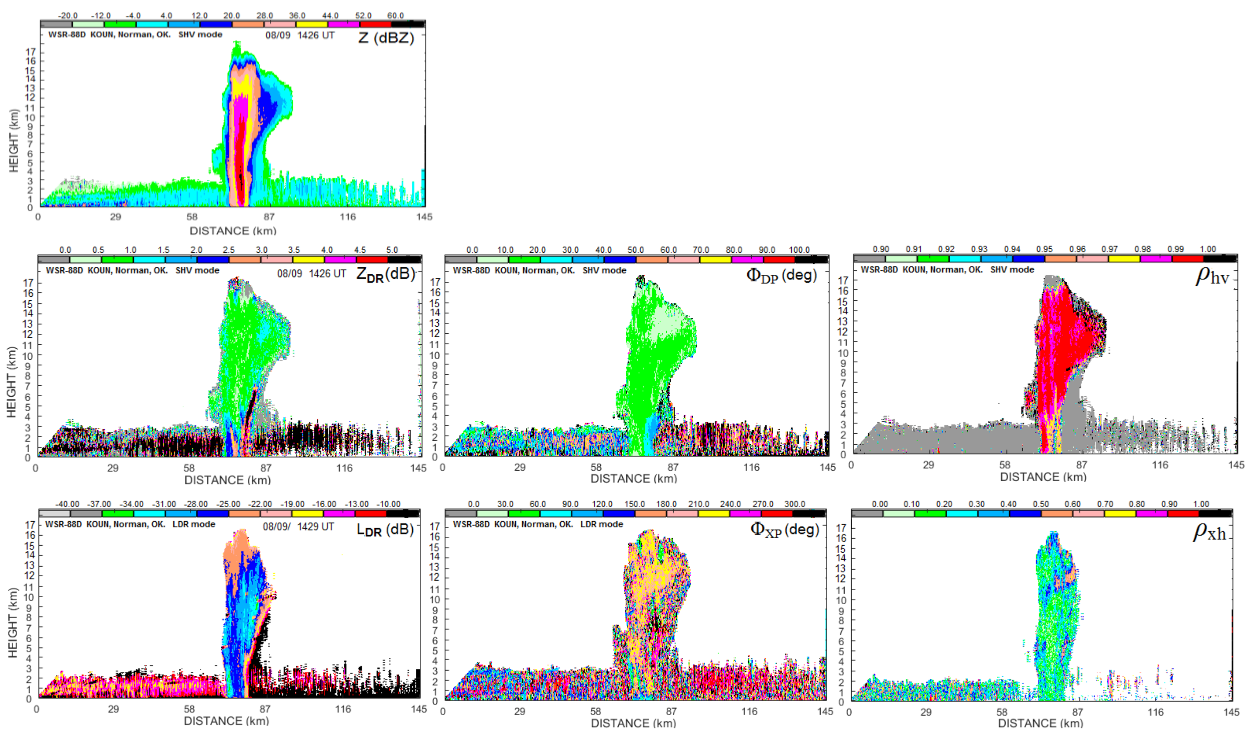

Fig.2. RHIs collected on 9 August 2007 at 1426 UTC at an azimuth of 330^{o}.

The second example is in Fig. 2, where Z_{DR} field has no pronounced features related to canted particles, whereas LDR mode shows a large area of enhanced L_{DR} at the top of the thunderstorm. The Φ_{DP} field allows for an assumption about the presence of canted particles in that area because of a decrease in values with range along the radar radials, but this could also be caused by particles' habits. The Φ_{XP} and ρ_{xh} fields undoubtedly point to canted particles. The ρ_{hv} field is featureless.

One more example is presented in Fig. 3, where Z_{DR} fields cannot undoubtedly reveal the canted particles, which can be revealed in the L_{DR} field at the top of thunderstorm. The Φ_{DP} field does not allow for conclusion about canted particles: the values gradually increase with range, which is a typical pattern of attenuation. The Φ_{XP} field exhibits large areas of uniform areas, which point to the presence of canted particles. The ρ_{hv} field is featureless, whereas ρ_{xh} field has a large area of high values, which reveals canted particles.

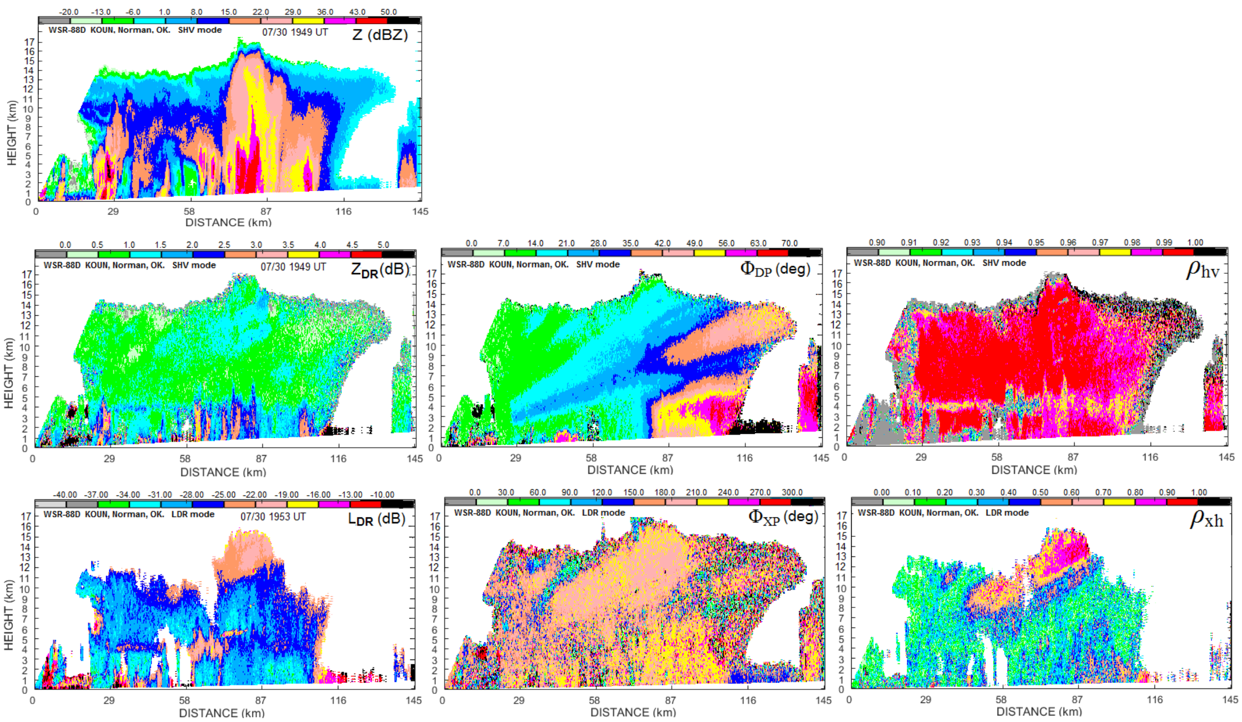

Fig. 3. RHIs collected on 30 July 2007 at 1949 UTC at an azimuth of 329°.

Radar fields in Figs. 1-3 allow for a conclusion that the LDR mode is more sensitive to canted particles that the SHV mode. So the LDR mode is advantageous in revealing cloud areas of canted particles. Such canting is caused by in-cloud electric fields.

The data in Figs. 1-3 were collected from summer thunderstorms. Areas of uniform Φ_{XP} and enhanced ρ_{xh} have been also observed by KOUN in winter storms. Two examples are shown in Figs. 4 and 5. In Fig. 4, the L_{DR} field is almost featureless in the area of convection, but the Φ_{XP} and ρ_{xh} fields reveal canted particles and therefore point to the presence of electric fields. The enhanced L_{DR} at heights 5-10 km at short distances from radar are most likely due to large stellar/dendrite particles. Similar conclusions can be drawn from Fig. 5, where the ρ_{xh} field has enhanced values in the area of convection (at 120- 150 km from radar) and in the stratiform area at distances of 30 – 50 km from radar.

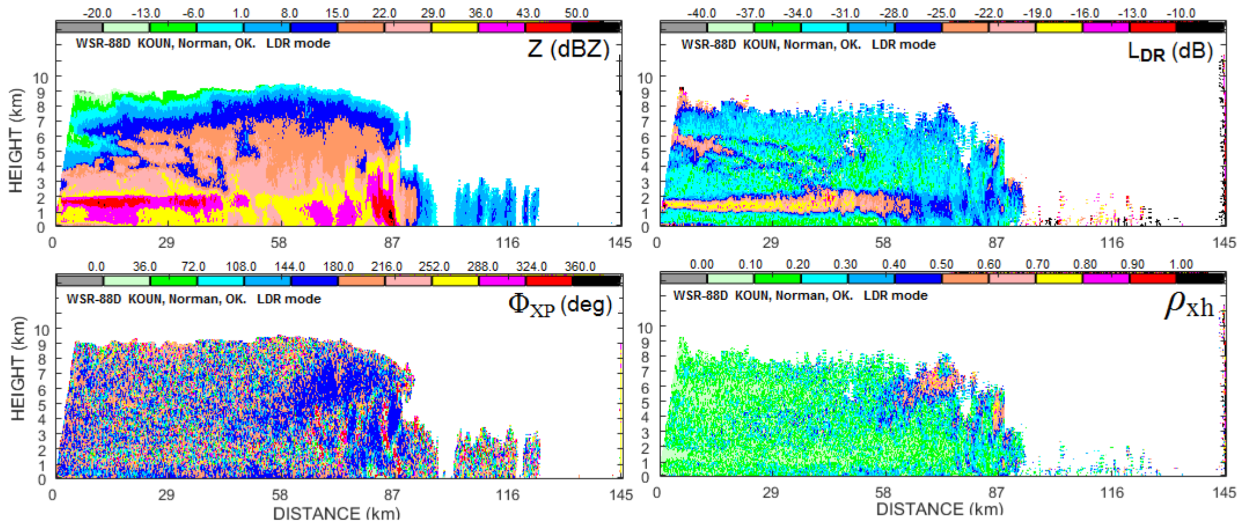

Fig. 4. RHIs in the LDR mode collected on 27 December 2008 at 1152 UTC at an azimuth of 260^o.

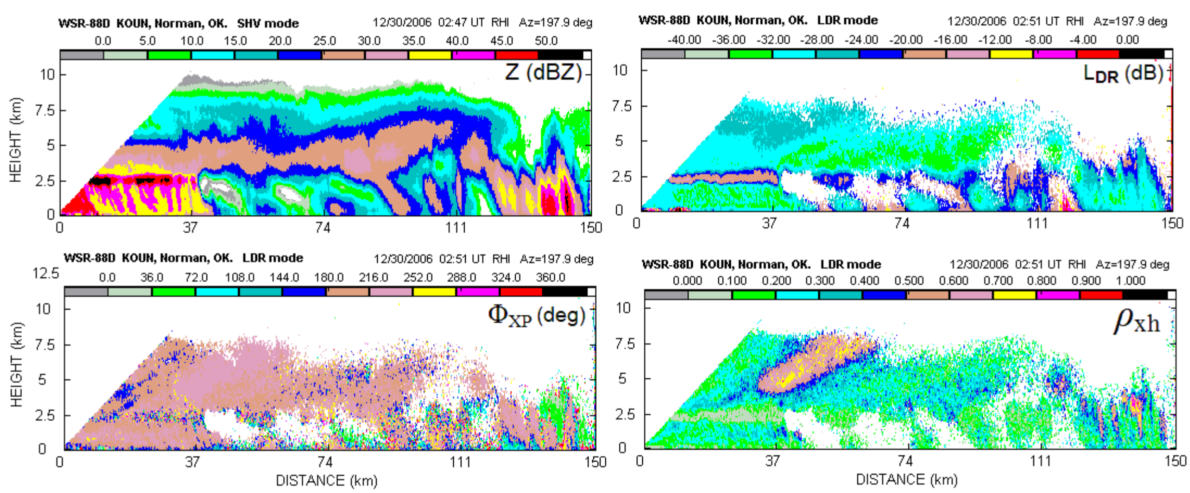

Fig. 5. RHIs in the LDR mode collected on 30 December 2006 at 0251 UTC at an azimuth of 198^o.

Conclusions

Polarimetric variables of the LDR mode are more sensitive to aligned ice crystal than those of the SHV mode and therefore the LDR mode is more advantageous in revealing electrified cloud areas. We also can submit that radar with circular polarization is more sensitive to depolarization by ice crystals than that operating in the SHV mode.

The system differential phase in transmit in the WSR-88D radars is not controlled and can deviate from zero. For instance in KOUN, this phase was about 27^o in 2015. Quality of data from the WSR-88Ds seems to be independent from the system differential phase in transmit. Circular polarization in transmit can be implemented on the WSR-88D and this could not affect the quality of polarization variables if a 90^o phase shift between horizontally and vertically polarized waves is introduced in receive. So to have both circularly and elliptically/linearly polarized signals, two separate receive channels could be introduced in the radar by shifting the phase in one of the channels by 90^o. Operational advantages of such a scheme could be verified by using existing dual polarization radars.

References

Biggerstaff, M., Z. Zounes, A. Alford, G. Carrie, J. T. Pilkey, M. Uman , and D. Jordan: 2017: Flash propagation and inferred charge structure relative to radar-observed ice alignment signatures in a small Florida mesoscale convective system. *J. Geophys. Res. Lett.* DOI: 10.1002/2017GL074610.

Caylor I.J., V. Chandrasekar, V.N. Bringi, and S.S. Minger, 1993: Multiparameter radar observations of lightning. *Prepr. 26th Weather Radar Conf.*, AMS, Boston, 306-308.

Caylor I.J., and V. Chandrasekar, 1996: Time-varying ice crystal orientation in thunderstorms observed with multiparameter radar. *IEEE Trans.* **GRS-34**, 847-858.

Furuta, O., H. Yuki, and M. Yamada: 1985: Abrupt changes in cross polarization observed during thunder. *IEEE Trans*., **AP-33**, n.6, 625-632.

Hendry A., and G. C. McCormick, 1976: Radar observation of the alignment of precipitation particles by electrostatic fields in thunderstorms. *J. Geophys. Res.*, **81**, 5353-5357.

Hendry, A., and Y.M.M. Antar, 1982: Radar observations of polarization characteristics and lightning-induced realignment of atmospheric ice crystals. *Radio Sci.*, **17**, 1243 – 1250.

Hubbert, J.C., S.M. Ellis, W.-Y. Chang, S. Rutledge, and M. Dixon, 2014: Modeling and Interpretation of S-Band Ice Crystal Depolarization Signatures from Data Obtained by Simultaneously Transmitting Horizontally and Vertically Polarized Fields. *J. Applied Meteorol. Climat.* **53**, 1659-1677.

Hubbert, J.C., S.M. Ellis, W.-Y. Chang, and Y.-C. Liou. X-Band Polarimetric Observations of Cross Coupling in the Ice Phase of Convective Storms in Taiwan. *J. Applied Meteorol. Climat.* **53**,1678-1695.

Krehbiel, P.R., W. Rison, S. McCrary, T. Blackman, and M. Brook, 1991: Dual-polarization radar observations of lightning echoes and precipitation alignment at 3-cm wavelength. *Prepr. 25th Weather Radar Conf.*, AMS, Boston, 901-904.

Krehbiel, P.R., T. Chen, S. McCrary, W. Rison, G. Gray, T. Blackman, and M. Brook, 1992: Dual polarization radar signatures of the potential for lightning in electrified storms. *9th Int. Conf. Atmos. Elect.*, St. Petersburg, Russia, 166-169.

Krehbiel, P.R., T. Chen, S. McCrary, T. S. McCrary, W. Rison, G. Gray, T. Blackman, and M. Brook, 1996: The use of dual polarization radar for remotely sensing storm electrification. *Meteorol. And Atmosph. Phys*. **59**, 65-82.

Melnikov, V., T. Schuur, and A. Ryzhkov, 2009: Recognition of lightning echoes with the polarimetric WSR-88D. Available online at: https://ams.confex.com/ams/34Radar/webprogram/Paper155320.html

Metcalf, J.I., 1995: Radar observations of changing orientations of hydrometeors in thunderstorms. *J. Applied Meteorol.*, **34**, 757-772.

Ryzhkov, A., and D. Zrnic, 2007: Depolarization in Ice Crystals and Its Effect on Radar Polarimetric Measurements, *J. Atmos. Oceanic Technol*. **24**, 1256-1267.

Weber, M., D. Zrnic, and P. Zhang, 2017: High Temporal-Resolution Monitoring of Ice Crystal Alignment. 97-th Annual AMS meeting. Seattle, WA . Available online at: https://ams.confex.com/ams/97Annual/webprogram/Paper309454.html